($\sigma = 0.1, \sigma = 0.2$ and $\sigma = 0.3$) at two critical points $z = 0.7$ And $z = 2.1$. As seen in Figure 5a, the axial velocity decreases with an increase in stenotic value at $z = 0.7$. Figure 5b shows an opposite behavior in the case of aneurysm. According to Figure 5b, the axial velocity increases with an increase in aneurysm value. These results agree closely with the observations of Lorenzini and Casalena [26] which they concluded that the blood flow peak velocities depend on the height of stenosis.

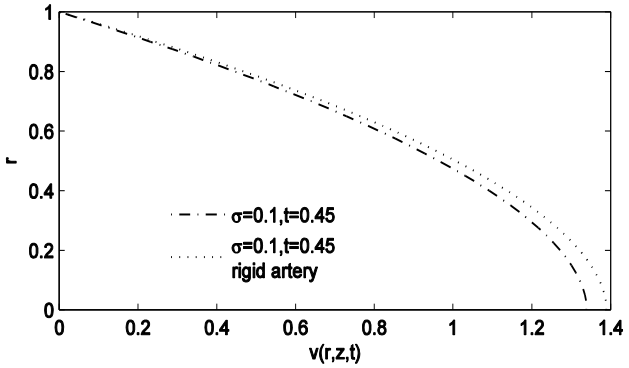

Figure 4. The axial velocity of radial variation

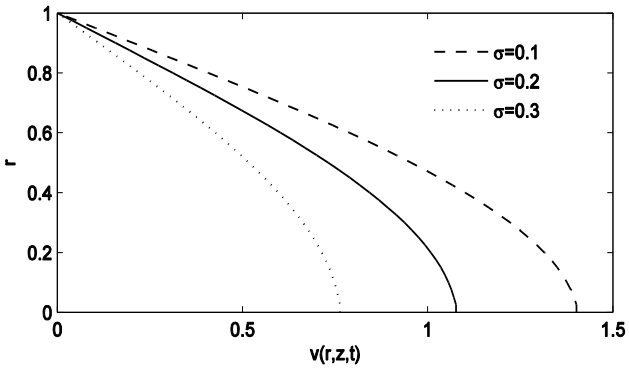

(a)

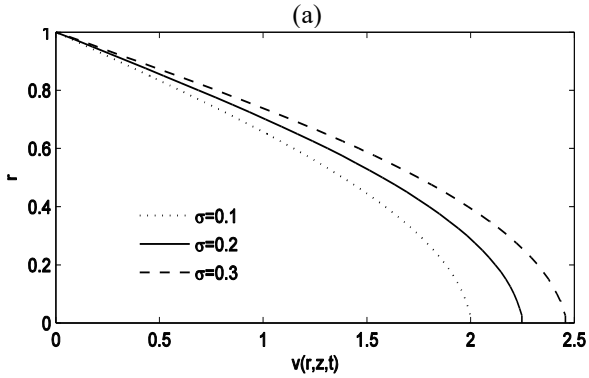

(b)

Figure 5. The dimensionless axial velocity profile for different values of stenotic and aneurysm

Figure 6 provides the axial velocity pattern of the artery against different tapered angles of aneurysm and stenotic. Figure 6 pointed on this fact that the axial velocity inside the artery has an increasing pattern against the increasing angle. Also, the result of non-tapered artery is located between the convergent and divergent tapered arteries curves. These results agree closely with the observations of Lorenzini and Casalena [26] which they concluded that the blood flow velocity and recirculation are strongly affected by the stenotic slope. Figure 7 shows the effect of Prandtl number on the temperature distributions inside the artery. This figure shows that the heat transfer rate will decrease with increase in the Prandtl number. In other words, the rate of heat transferred from the artery to the blood decreases with increase in the Prandtl number.

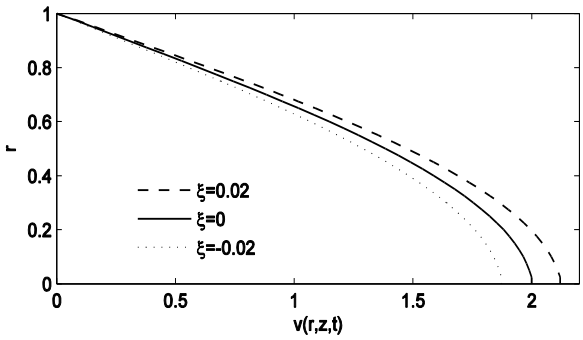

Figure 6. The dimensionless axial velocity profile for different tapered angles

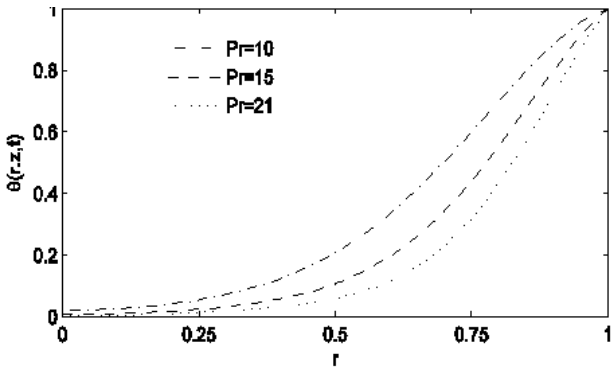

Figure 7. The dimensionless temperature profile for different prandtl numbers

Figure 8 denotes the variation of Br against the dimensionless temperature profile. It can be seen that the temperature of crossing blood increases with increases in the Br value. Also, it can be seen that when Br increases the heat transfer decreases as the result of temperature increasing.

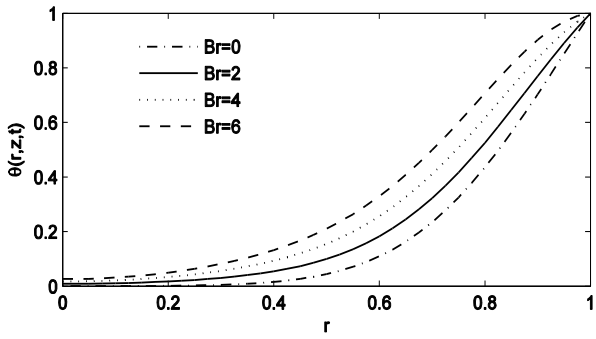

Figure 8. The dimensionless temperature profile for different prandtl numbers

Figure 9 the effect of body acceleration (D_2) on the non-Newtonian flow rate (blood) is described in Figure 9. Figure 9a declares that the blood flow is strongly up to the acceleration of the body. When D_2 is increased slowly, the maximum velocity develops sooner. Since the axial velocity

of the blood flow and the volumetric rate are in a close relationship, the flow rate will increase with improvement in the body acceleration parameter. Figure 9b shows that the profiles of the flow rate which changes against the time. As a result, comparison between three different values of stenosis/aneurysms leads to this point; increase in the aneurysm value can result a significant enhance in the volumetric flow rate. (The graph shows the pulse behavior blood flow in different heartfelt periods).

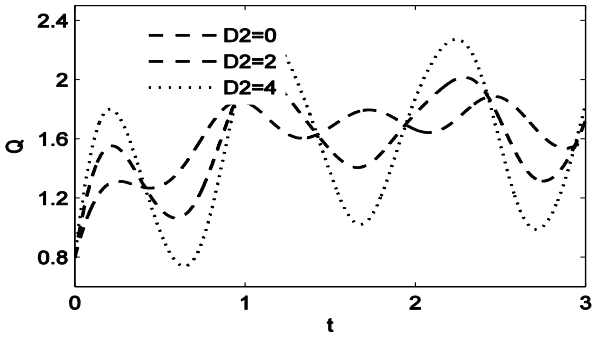

(a)

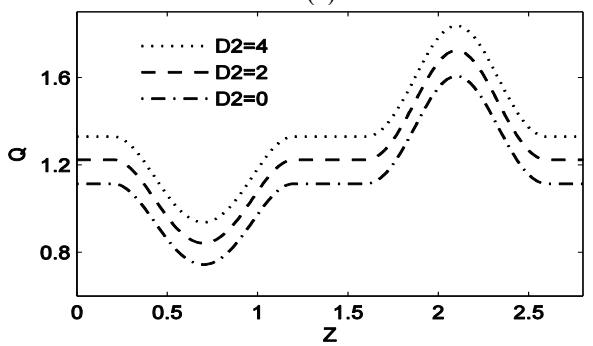

(b)

Figure 9. The flow rate profile for different acceleration values

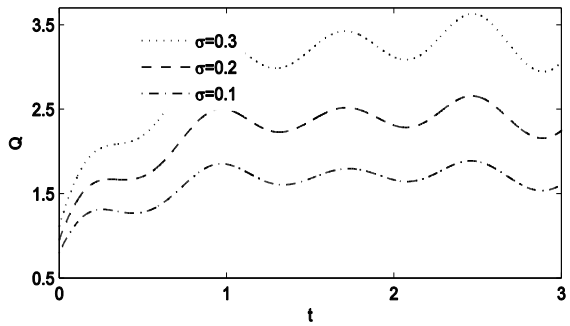

(a)

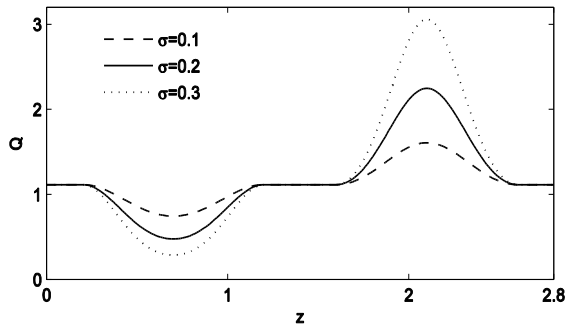

(b)

Figure 10. The Flow rate profile for different values of aneurysm

Figure 10a shows the effect of body acceleration parameter on the blood flow inside the considered artery. As said before, the acceleration of body and the blood flow rate are directly related to each other, so, when the velocity increases, the flow rate increases too. Figure 10b describes the effect of aneurysms/ stenotic size on the blood flow against the position and place. When the aneurysms size increases the flow rate improves and consequently the blood velocity increases.

Figure 11 illustrates the effect of Weissenberg number (as a dimensionless number at different times) on dimensionless blood flow rate. In can be visible that the blood flow rate will reduce with the increasing Weissenberg number. As another result, the patterns or treatments of volumetric flow rates for the Weissenberg numbers are related to the geometry of the stenosis and aneurysms.

Figure 12 the effect of Reynolds number on the blood flow resistance is indicated in Figure 11. This figure illustrates that when the Reynolds number increases the resistance against the blood flow increases. In other words, the pressure drop enhances with the increasing velocity.

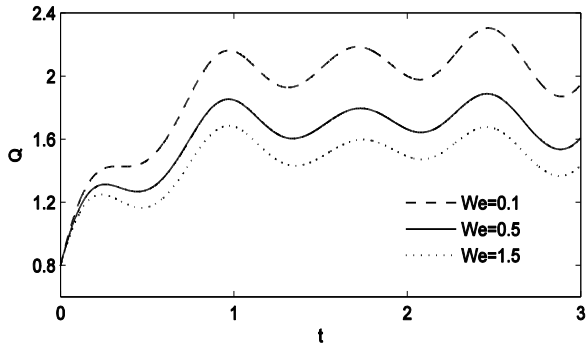

Figure 11. The flow rate profile for different Weissenberg number

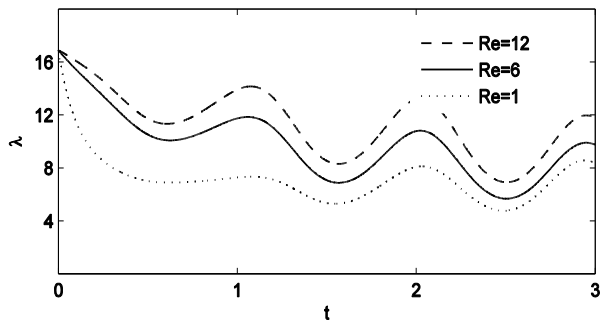

Figure 12. The resistance to flow profile for different Reynolds number

Figure 13 tries to declare the impact of dimensionless Weissenberg number we at different times on dimensionless impedance. As shown in Figure 12, the enhancing Weissenberg number can create an important increase in impedance. Also, in can be understood that the volumetric flow rate plays an opposite role against the blood flow resistance.

Figure 14 indicates the flow resistance different time series for different Power law indexes. According to these results, increase in the Power law index leads to decrease in the blood flow resistance, or in other words, blood flow resistance decreases with the increasing n parameter.

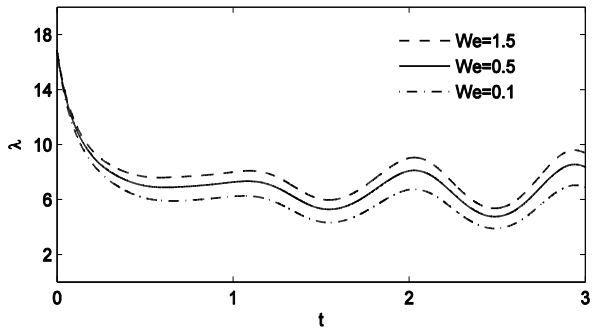

Figure 13. The resistance impedance profile for different Weissenberg number

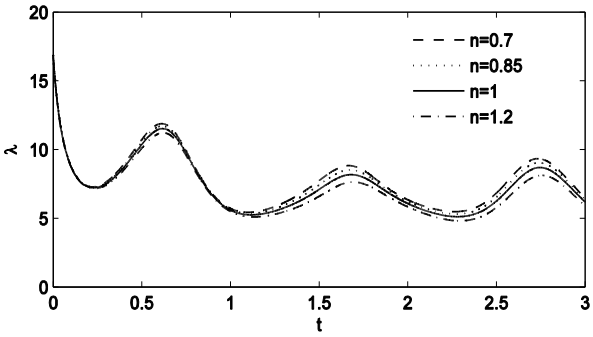

Figure 14. The resistance impedance profile for different power low index

Figure 15 the impact of Reynolds number on the wall shear stress is presented in Figure 15. This figure states that the wall shear stress can be increased when the related Reynolds number increases.

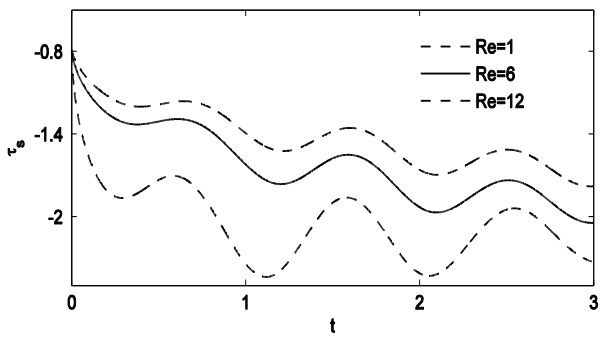

Figure 15. The wall shear stress profile for different Reynolds number

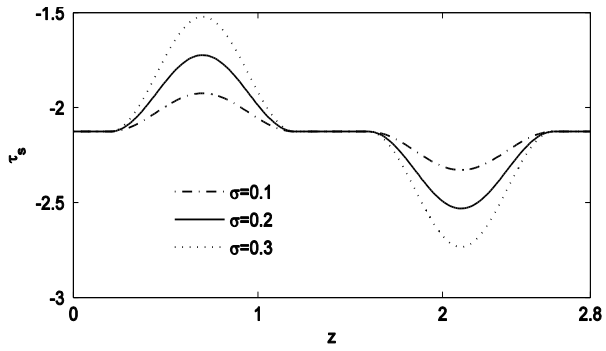

Figure 16. The wall shear stress profile for different values

Figure 16 based on the results of Figure 16 (at $Z = 2.1$), when the size of stenosis grows the wall shear stress increases. Furthermore, when the size of aneurysms increases the wall shear stress decreases.

Figure 17 points on the wall shear stress values for tapered and non-tapered arteries in geometry. As seen in this figure, the wall shear stress allays when the angle tapered increases. Also, it can be observed that the trend for non-tapered artery is located between the curves belong to the convergent and divergent arteries.

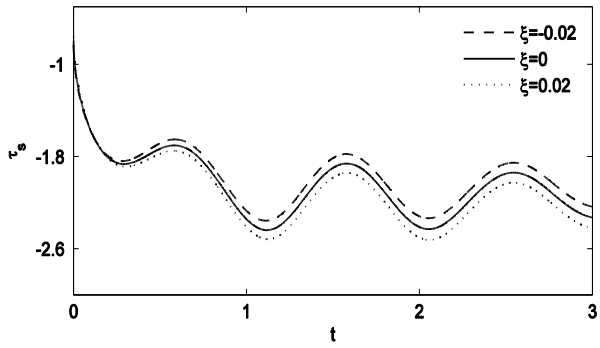

Figure 17. The wall shear stress profile for different tepered angles

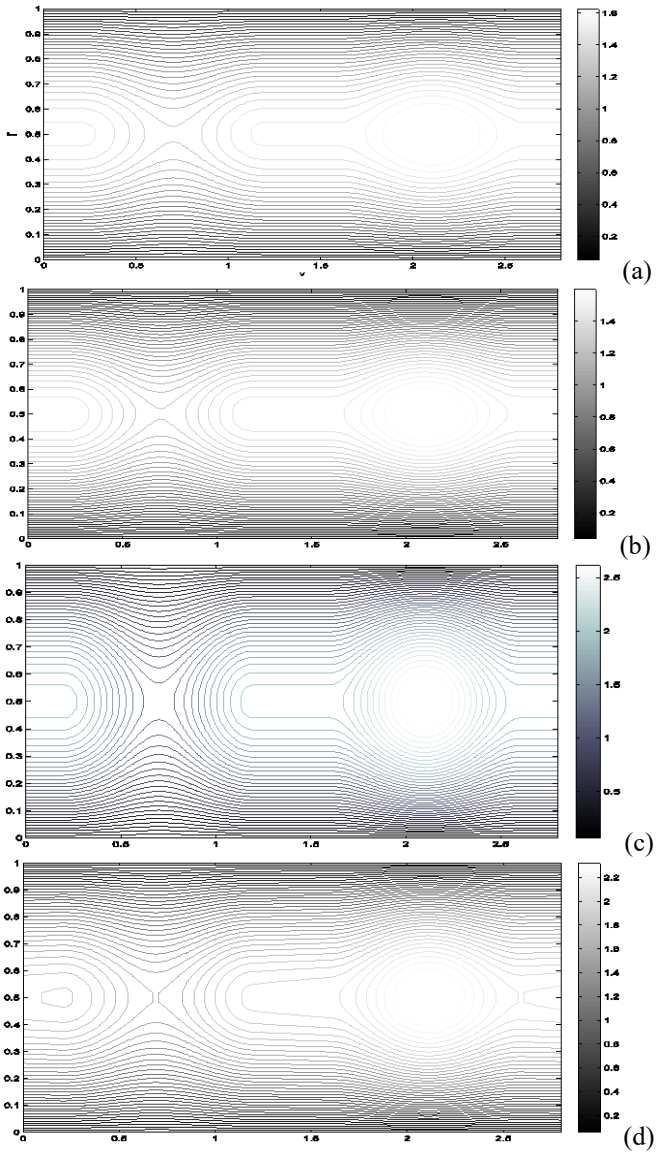

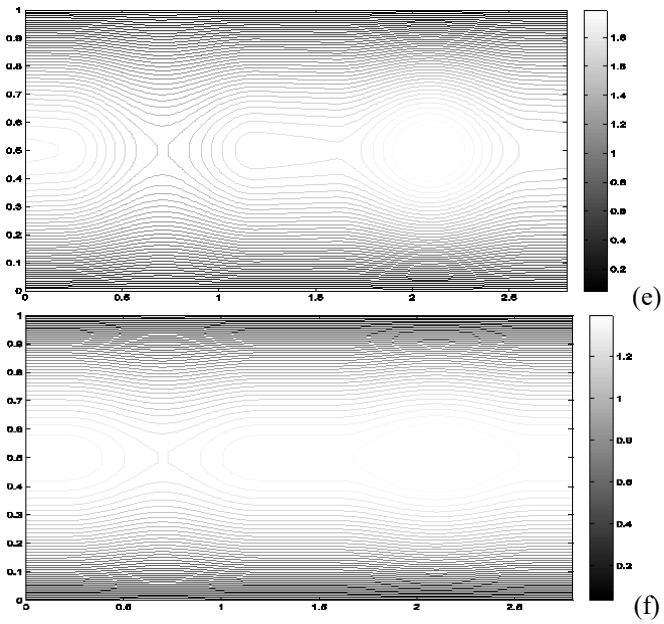

Figure 18. Contour of velocity of blood flow

Figure 18 the patterns and behaviors of the blood flow for different values of We, τ, ξ, D_2 and Re are shown in Figure 18. Figure 18a shows a contour for some fixed parameters. By comparing plans a and b we found that when the Weissenberg number increases, the power of blood decreases. Besides, when the size of stenosis increases the blood flow velocity reduces and in the case of aneurysms, the velocity increases with increase in the height of aneurysms (comparing plans (a) and (c)). Furthermore, this comparison shows that in the non-tapered artery (left side) a small vortex is formed. In the systole phase the behavior is a little different from the diastolic phase. The effect of acceleration parameter on the blood flow is visible in the comparison view between plans (a) and (e). As said before, the flow velocity will increase with an improving acceleration. The effect of Reynolds number can be seen in plan (f). Also, when the Reynolds number is increased the flow rate on the arterial axis allays (the blood flow is reduced near the artery walls).

The two dimensional temperature distributions for some specific parameters are shown in Figure 19. The plan (a) has been compared to other plans in as a function of τ , Br, We and sigma. As seen in comparison of plans (a) and (b), the temperature reduces when we have an increase the amount of stenosis and aneurysm. As another result, the increase in Brinkman and Weissenberg numbers leads to some positive and negative effects on the temperature values, reflectively (plans (a), (c) and (d)). The comparison between plans (a), (e) and (f) describes the effects of taper angle (divergent and convergent arteries) on the temperature profiles.

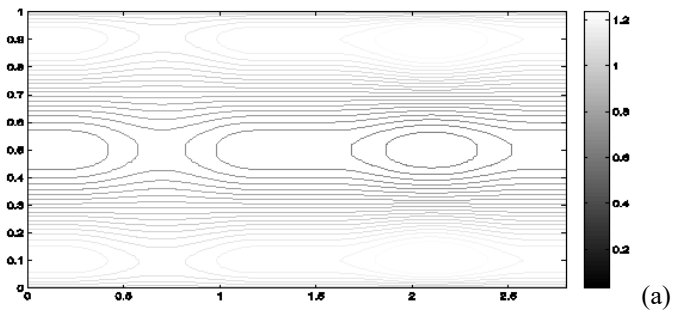

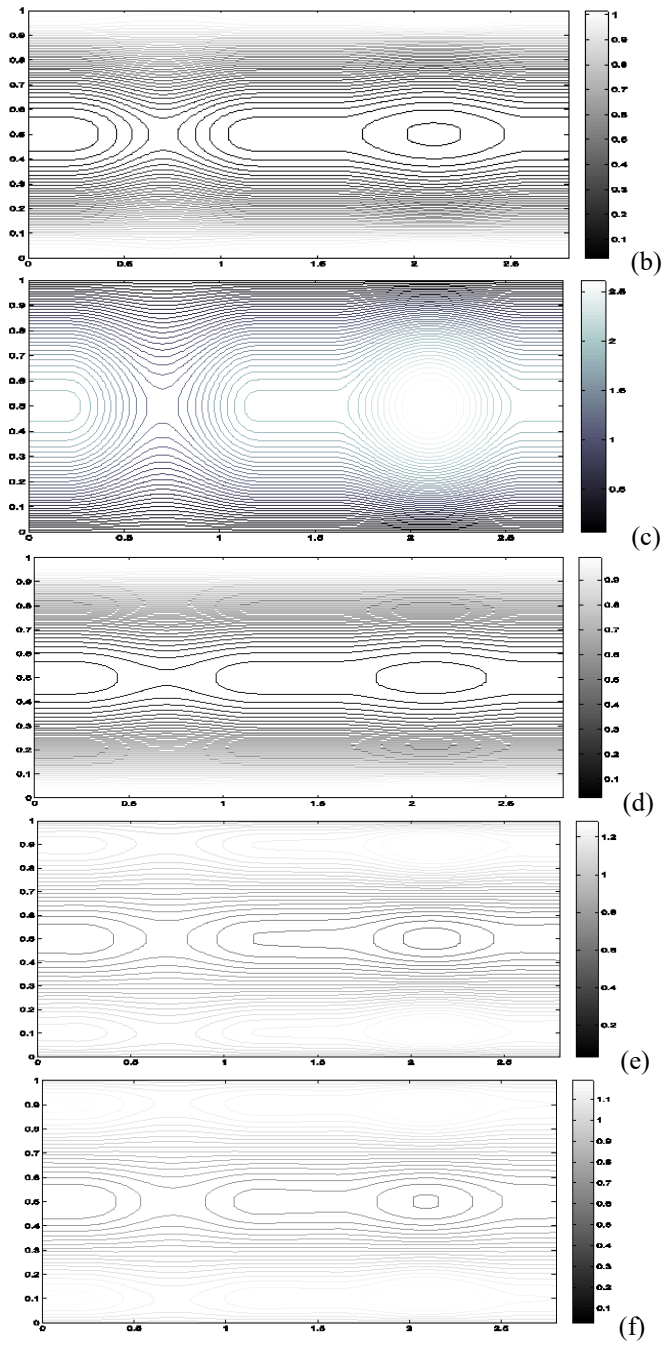

Figure 19. The contour of temperature of blood flow

7. CONCLUSION

In this investigation the blood flow patters and the effects of heat transfer between the wall of arteries and the flow on the blood characteristics have been studied. The mentioned parameters on a cross section area of the arteries in the axial direction have been analyzed in different situations. The velocity and temperature distributions are investigated as two main affective parameters on the blood flow. The Blood flow is assumed to have some conditions near the real state such as pulsed, nonlinear, layered and unstable and flowing through an elastic wall. The comparison between the present simulation and previous works shows a good agreement which proves the accuracy of the results. We also provided some comparisons between our results and those of Lorenzini and Casalena [26] who analyzed the blood flow in a coronary artery, affected by different stenotic shapes, via a CFD code.

The results prove that when the Prandtl and Brinkman numbers increase, the heat transfer between the blood and the artery walls and the temperature values on the profiles {improve}. By comparing the elastic and the rigid walls, it can be seen that the axial velocity of elastic wall is less than the axial velocity regarding the rigid wall. Furthermore, when the aneurysm size is increased the axial velocity and the flow rate will be increased.

REFERENCES

[1] Mortazavinia Z, Zare A, Mehdizadeh A. (2012). Effects of renal artery stenosis on realistic model of abdominal aorta and renal arteries incorporating fluid-structure interaction and pulsatile non-Newtonian blood flow. Applied Mathematics and Mechanics 33(2): 165-176. http://dx.doi.org/10.1007/s10483-012-1541-6

[2] Mandal PK. (2005). An unsteady analysis of non-Newtonian blood flow through tapered arteries with a stenosis. International Journal of Non-Linear Mechanics 40(1): 151-164. https://doi.org/10.1016/j.ijnonlinmec.2004.07.007

[3] Haghighi AR, Pralhad RN. (2009). Mathematical modelling of blood flows under the effects of body forces and magnetism on human body. International Journal of Biomedical Engineering and Technology 2(4): 295-302. http://dx.doi.org/10.1504/IJBET.2009.027794

[4] Mekheimer KS, El Kot MA. (2008). The micropolar fluid model for blood flow through a tapered artery with a stenosis. Acta Mechanica Sinica 24(6): 637-644. http://dx.doi.org/10.1007/s10409-008-0185-7

[5] Pontrelli G. (1998). Pulsatile blood flow in a pipe. Computers & Fluids 27(3): 367-380. https://doi.org/10.1016/S0045-7930(97)00041-8

[6] Lee JS, Fung YC. (1970). Flow in locally constricted tubes at low Reynolds numbers. Journal of Applied Mechanics 37(1): 9-16. https://doi.org/10.1115/1.3408496

[7] Azuma T, Fukushima T. (1976). Flow patterns in stenotic blood vessel models. Biorheology 13(6): 337-355. https://doi.org/10.3233/BIR-1976-13602

[8] Liu GT, Wang XJ, Ai BQ, Liu LG. (2004). Numerical study of pulsating flow through a tapered artery with stenosis. Chinese Journal of Physics 42(4): 401-409. https://doi.org/10.6122/CJP

[9] Ismail Z, Abdullah I, Mustapha N, Amin N. (2008). A power-law model of blood flow through a tapered overlapping stenosed artery. Applied Mathematics and Computation 195(2): 669-680. https://doi.org/10.1016/j.amc.2007.05.014

[10] Akbar NS, Nadeem S. (2014). Carreau fluid model for blood flow through a tapered artery with a stenosis. Ain Shams Engineering Journal 5(4): 1307-1316. https://doi.org/10.1016/j.asej.2014.05.010

[11] Zaman A, Ali N, Sajid M, Hayat T. (2015). Effects of unsteadiness and non-Newtonian rheology on blood flow through a tapered time-variant stenotic artery. AIP Advances 5(3): 037129. https://doi.org/10.1063/1.4916043

[12] Rathod VP, Tanveer S, Rani IS, Rajput GG. (2006). Pulsatile flow of blood with periodic body acceleration and magnetic field through an exponentially diverging vessel. Ultra Sci. Phys. Sci. 18: 417-426.

[13] Burton RR, Leverett JS, Michaelson ED. (1974). Man at high sustained Gz acceleration: A review, Aerospace Medicine 45(10): 1115-1136.

[14] Chakravarty S, Sannigrahi AK. (1998). An analytical estimate of the flow-field in a porous stenotic artery subject to body acceleration. International Journal of Engineering Science 36(10): 1083-1102. https://doi.org/10.1016/S0020-7225(98)00009-3

[15] Haghighi AR, Asl MS. (2015). Mathematical modeling of micropolar fluid flow through an overlapping arterial stenosis. International Journal of Biomathematics 8(04): 1550056. https://doi.org/10.1142/s1793524515500564

[16] Zaman A, Ali N, Bég OA. (2016). Numerical simulation of unsteady micropolar hemodynamics in a tapered catheterized artery with a combination of stenosis and aneurysm. Medical & Biological Engineering & Computing 54(9): 1423-1436. https://doi.org/10.1007/s11517-015-1415-3

[17] Shit GC, Majee S. (2015). Pulsatile flow of blood and heat transfer with variable viscosity under magnetic and vibration environment. Journal of Magnetism and Magnetic Materials 388: 106-115. http://dx.doi.org/10.1016/j.jmmm.2015.04.026

[18] Eldabe NT, Moatimid GM, Hassan MA, Mostapha DR. (2016). Effects of partial slip on peristaltic flow of a Sisko fluid with mild stenosis through a porous medium. Appl. Math. Inf. Sci. 10(2): 673-687. http://dx.doi.org/10.18576/amis/100227

[19] Zaman A, Ali N, Bég OA, Sajid M. (2016). Heat and mass transfer to blood flowing through a tapered overlapping stenosed artery. International Journal of Heat and Mass Transfer 95: 1084-1095. https://doi.org/10.1016/j.ijheatmasstransfer.2015.12.073

[20] Mekheimer KS, Haroun MH, El Kot MA. (2012). Influence of heat and chemical reactions on blood flow through an anisotropically tapered elastic arteries with overlapping stenosis. Appl. Math 6(2): 281-292.

[21] Mekheimer KS, El Kot MA. (2012). Mathematical modelling of unsteady flow of a Sisko fluid through an anisotropically tapered elastic arteries with time-variant overlapping stenosis. Applied Mathematical Modelling 36(11): 5393-5407. https://doi.org/10.1016/j.apm.2011.12.051

[22] Sankar DS, Lee U. (2011). Nonlinear mathematical analysis for blood flow in a constricted artery under periodic body acceleration. Communications in Nonlinear Science and Numerical Simulation 16(11): 4390-4402. https://doi.org/10.1016/j.cnsns.2011.03.020

[23] Chakravarty S, Mandal PK. (2009). Effect of heat and mass transfer on non-Newtonian flow–Links to atherosclerosis. International Journal of Heat and Mass Transfer 52(25-26): 5719-5730. https://doi.org/10.1016/j.ijheatmasstransfer.2009.04.040

[24] Victor SA, Shah VL. (1975). High transfer to blood flowing in a tube. Biorheology 12: 361. https://doi.org/10.3233/BIR-1975-12606

[25] Zaman A, Ali N, Bég OA. (2016). Numerical study of unsteady blood flow through a vessel using Sisko model. Engineering Science and Technology, an International Journal 19(1): 538-547. https://doi.org/10.1016/j.jestch.2015.09.013

[26] Lorenzini G, Casalena E. (2008). CFD analysis of

pulsatile blood flow in an atherosclerotic human artery with eccentric plaques. Journal of Biomechanics 41(9): 1862-1870. https://doi.org/10.1016/j.jbiomech.2008.04.009

[27] Haghighi AR, Kabdool AA, Asl MS. (2016). Numerical investigation of pulsatile blood flow in stenosed artery. International Journal of Applied and Computational Mathematics 2(4): 649-662. http://dx.doi.org/10.1007/s40819-015-0084-0

[28] Haghighi AR, Asl MS, Kiyasatfar M. (2015). Mathematical modeling of unsteady blood flow through elastic tapered artery with overlapping stenosis. Journal of the Brazilian Society of Mechanical Sciences and Engineering 37(2): 571-578. https://doi.org/10.1007/s40430-014-0206-3

[29] Haghighi AR, Aliashrafi N. (2018). Mathematical modeling of pulsatile blood flow and heat transfer under magnetic and vibrating environment. International Journal of Heat and Technology 36(3): 783-790. https://doi.org/10.18280/ijht.360302

[30] Mabood F, Ibrahim ShM, Lorenzini G, Lorenzin E. (2017). Radiation effects on Williamson nanofluid flow over a heated surface with magnetohydrodynamics. International Journal of Heat and Technology 35(1): 196-204. http://dx.doi.org/10.18280/ijht.350126

[31] Haghighi AR, Chalak SA. (2017). Mathematical modeling of blood flow through a stenosed artery under body acceleration. Journal of the Brazilian Society of Mechanical Sciences and Engineering 39(7): 2487-2494. http://dx.doi.org/10.1007/s40430-017-0716-x

[32] Mustapha N, Mandal PK, Johnston PR, Amin N. (2010). A numerical simulation of unsteady blood flow through multi-irregular arterial stenoses. Applied Mathematical Modelling 34(6): 1559-1573. https://doi.org/10.1016/j.apm.2009.09.008

[33] Amsden AA, Harlow FH. (1970). The SMAC method: A numerical technique for calculating incompressible fluid flows. LA--4370. Los Alamos Scientific Laboratory Report LA-4370. United States.

[34] Markham G, Proctor MV. (1983). Modifications to the two-dimensional incompressible fluid flow code ZUNI to provide enhanced performance. C.E.G.B. Report TPRD/L/0063/M82. Leatherhead, England.

NOMENCLATURE

Br	Brinkman number
c_p	Specific heat
f_p	Pulse frequency
k_r	Oscillation parameter
L	Finite length of the arterial segment
l_0	Length of the stenosis
n	Power law index
p	pressure
P_r	Prandtl number
Q	Rate of flow
R(z)	Radius of the nonstenotic
Re	Reynolds number
S	Extra stress tensor
t	time
T	Temperature
u	Radial velocity
U_0	Average velocity
v	Axial velocity
We	Weissenberg number

Greek symbols

Δt	Time direction
Δz	Axial direction
$\Delta \kappa$	Radial direction
τ_s	Wall shear sterss
σ	Critical heigh
μ	Viscosity
Λ	Resistive impedance
φ	Phase angle

Subscripts

i
j
k